Supplementary Information

Truly tiny acoustic biomolecules for ultrasound diagnostics and therapy

Bill Ling[1], Bilge Gungoren[1], Yuxing Yao[1], Przemysław Dutka[1,2], Cameron A. B. Smith[1], Justin Lee[2], Margaret B. Swift[1], Mikhail G. Shapiro[1,3,4,*]

1. Division of Chemistry and Chemical Engineering, California Institute of Technology, Pasadena, CA, USA
2. Division of Biology and Bioengineering, California Institute of Technology, Pasadena, CA, USA
3. Division of Engineering and Applied Science, California Institute of Technology, Pasadena, CA, USA
4. Howard Hughes Medical Institute, California Institute of Technology, Pasadena, CA, USA

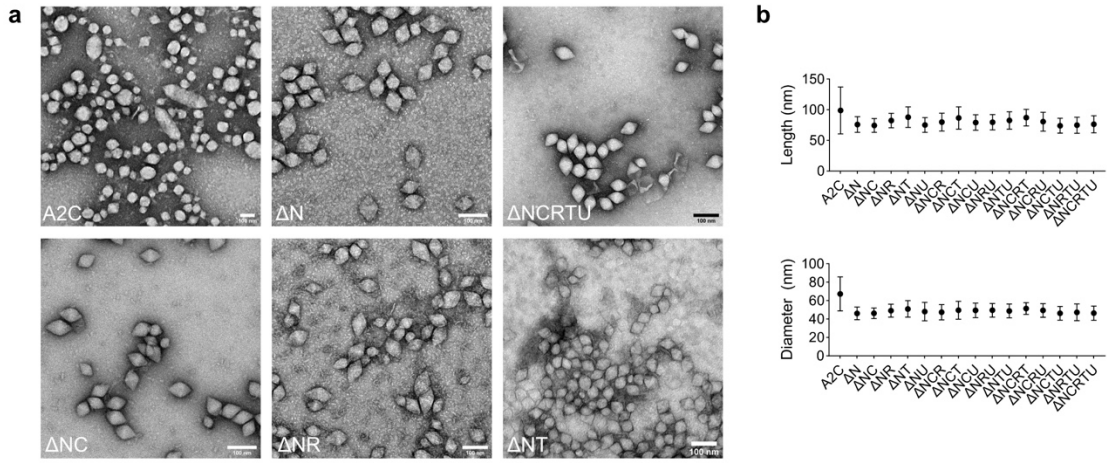

Figure S1. Impact of gene deletions on GV morphology. **a)** Representative TEM images of GVs expressed using the indicated gene cluster. A2C represents the full GV cluster[1]. Deletions are indicated by Δ. Scale bars, 100 nm. **b)** Mean length and diameter of individual particles measured in images from panel A. *N* = 50-100 particles. Error bars, ± SD.

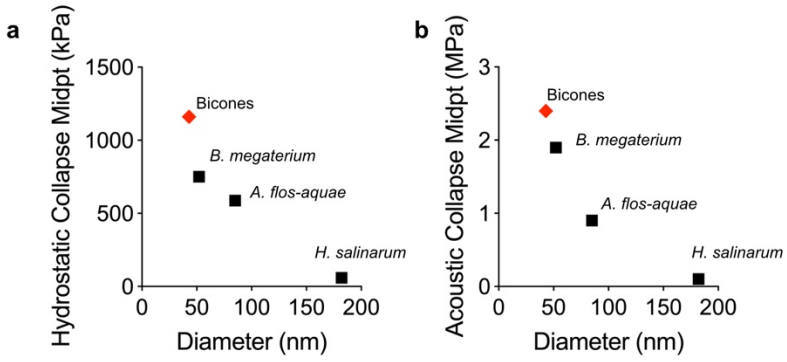

Figure S2. Comparison of hydrostatic (**a**) and acoustic (**b**) collapse midpoints for bicones relative to GVs isolated from *H. salinarum* and *A. flos-aquae*[2], or recombinantly expressed in *E. coli* using a cluster native to *B. megaterium*[3].

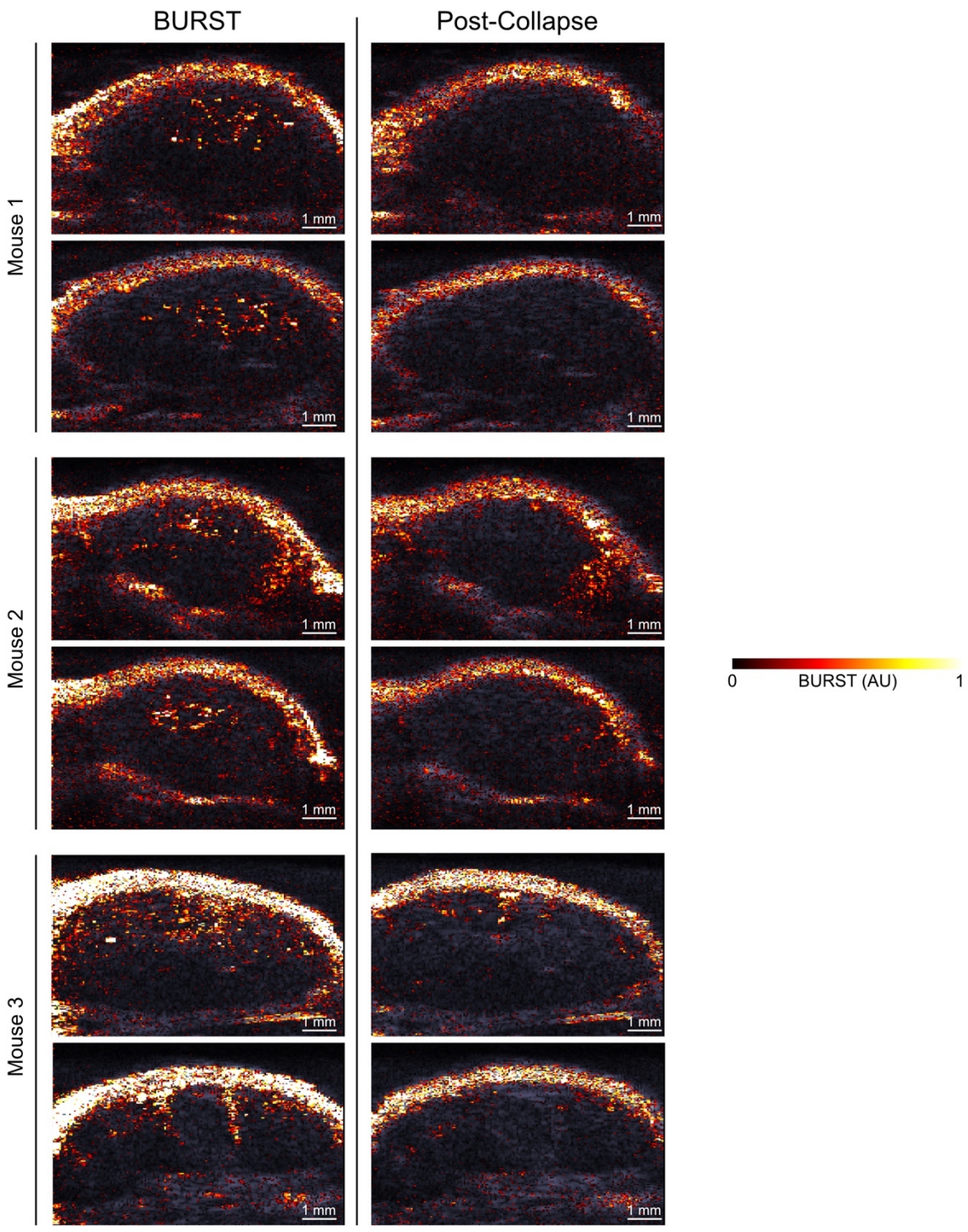

Figure S3. BURST images of U-87 MG tumors acquired 1 h after IV injection of bicones, overlaid on a B-mode image to show anatomy. A second acquisition (Post-Collapse) at the same location was used to verify that signal was specific to intact bicones. Two sets of images were acquired at different planes within each tumor. *N* = 3. Scale bars, 1 mm.

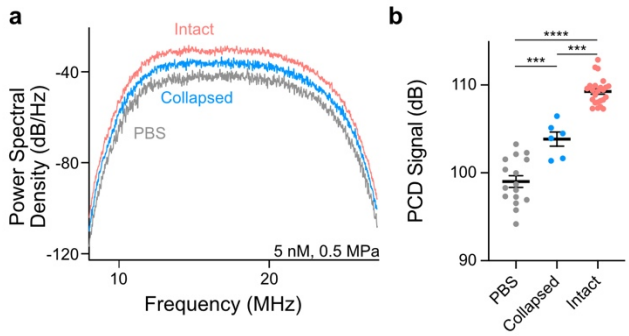

Figure S4. a) Representative power spectral density of emissions from PBS, pre-collapsed, and intact bicones (5 nM) insonated with a single 30 cycle FUS pulse at 0.5 MPa PNP. **b)** Mean PCD signal of samples from panel A, calculated by integrating spectra from 8 MHz to 27 MHz. PBS, *N* = 16; collapsed, *N* = 6; intact, *N* = 24. Error bars, ± SEM. Welch's t-test (***, p < 0.001; ****, p < 0.0001).

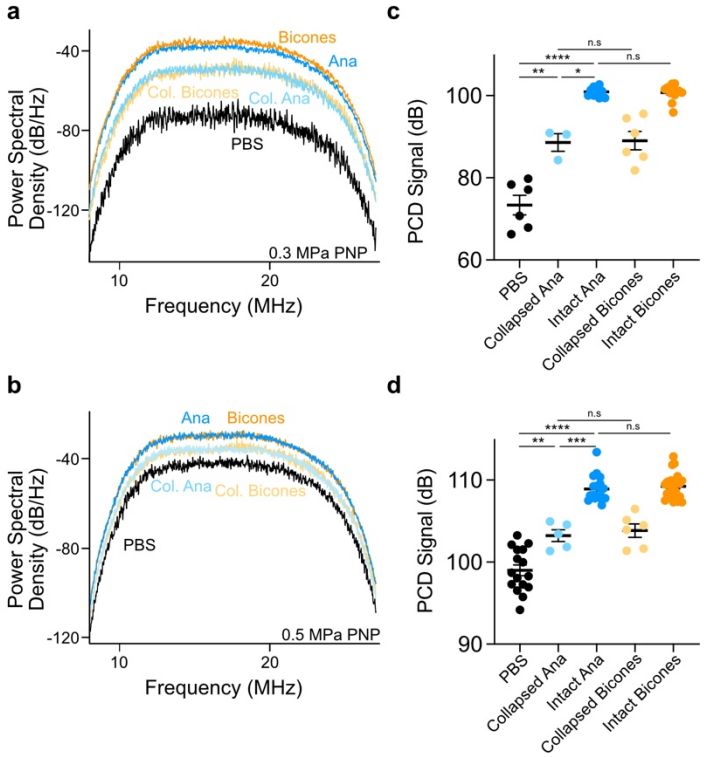

Figure S5. Bicones produce comparable PCD signal to *Anabaena* GVs at the same gas volume. **a-b)** Representative power spectral densities of acoustic emissions following insonation of bicones (4.2 nM) and *Anabaena* GVs (OD 0.25) with a single FUS pulse at 0.3 MPa PNP (**a**) or 0.5 MPa PNP (**b**). **c-d)** Mean PCD signal following insonation at 0.3 MPa PNP (**c**) or 0.5 MPa PNP (**d**). Spectra were integrated from 8-27 MHz. *N* = 3-24. Error bars, ± SEM. Welch's t-test, (*, p < 0.05; **, p < 0.01; ***, p < 0.001; ****, p < 0.0001; n.s, p ≥ 0.05).

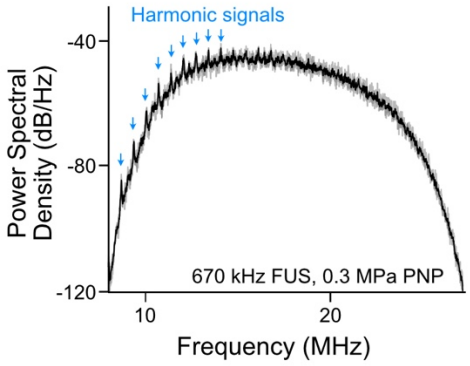

Figure S6. Power spectral density of emissions from intact bicones (5 nM) insonated with a single 60 cycle 670 kHz FUS pulse at 0.3 MPa PNP. *N* = 3. Individual trials are shown in gray, and the mean is shown in black. Harmonic signals indicative of stable cavitation are annotated with blue arrows.

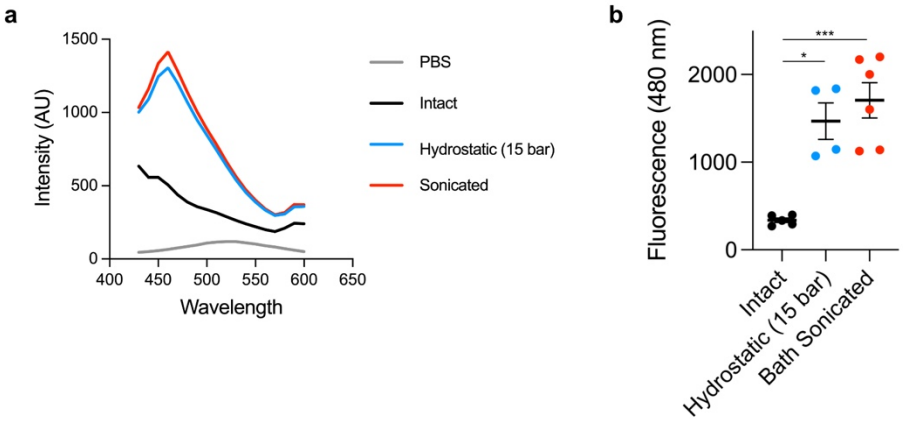

Figure S7. ANS fluoresces in the presence of collapsed bicones. **a)** Representative fluorescence emission spectra (ex. 380 nm) of bicone samples with 100 μM ANS following collapse by bath sonication or hydrostatic pressure. **b)** Fluorescence intensity at 480 nm in spectra from panel A. *N* = 4–6. Error bars, ± SEM. Welch's t-test (*, $p < 0.05$; ***, $p < 0.001$).

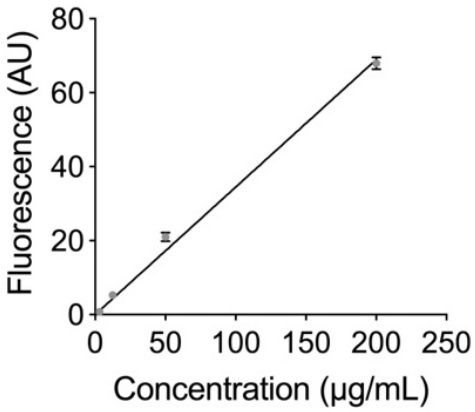

Figure S8. Fluorescence of suspensions containing 100 µM ANS mixed with the indicated concentration of collapsed bicones. Data were fit by linear regression, slope = 0.3447, r^2 = 0.99. *N* = 4. Error bars, ± SEM.

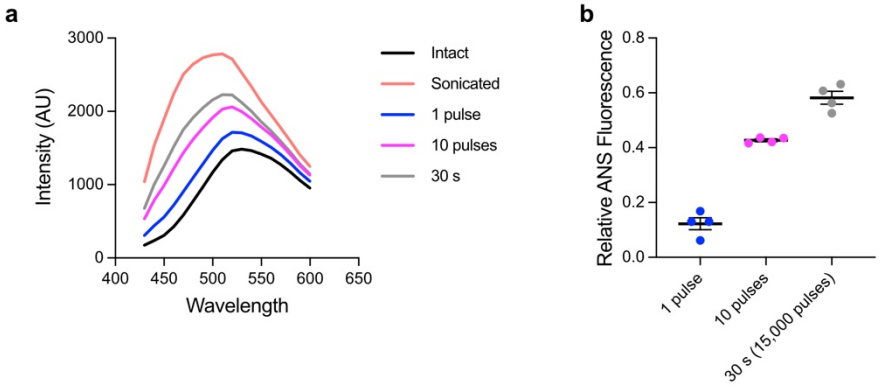

Figure S9. *Anabaena* GVs collapse under FUS insonation. **a)** Representative emission spectra of OD 0.25 *Anabaena* GVs with 100 µM ANS following insonation at 0.65 MPa PNP, 500 Hz pulse repetition frequency. **b)** Relative ANS fluorescence at 480 nm of GVs after exposure to 1, 10, or 15,000 FUS pulses at 0.65 MPa PNP, normalized to fluorescence of intact and pre-collapsed samples. *N* = 4. Error bars, ± SEM.

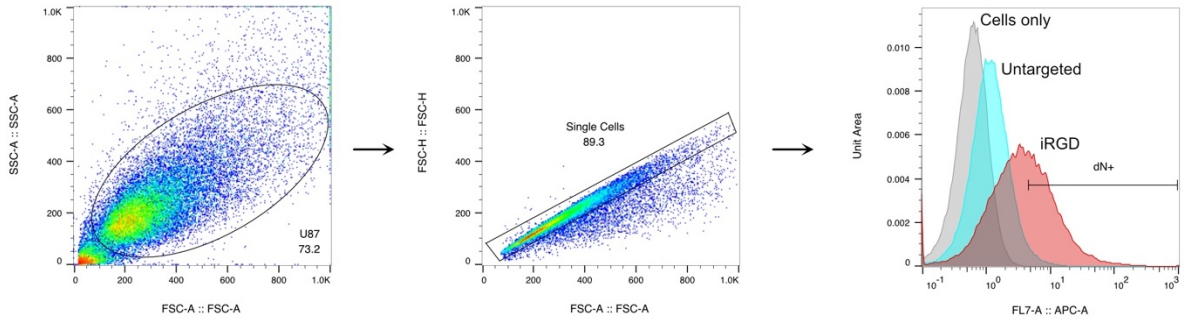

Figure S10. Flow cytometry gating strategy for iRGD targeting experiments. Debris was excluded based on SSC-A vs FSC-A. Single cells were selected from FSC-H vs FSC-A. Bicone positive cells (dN+) were defined relative to a cell-only control sample.

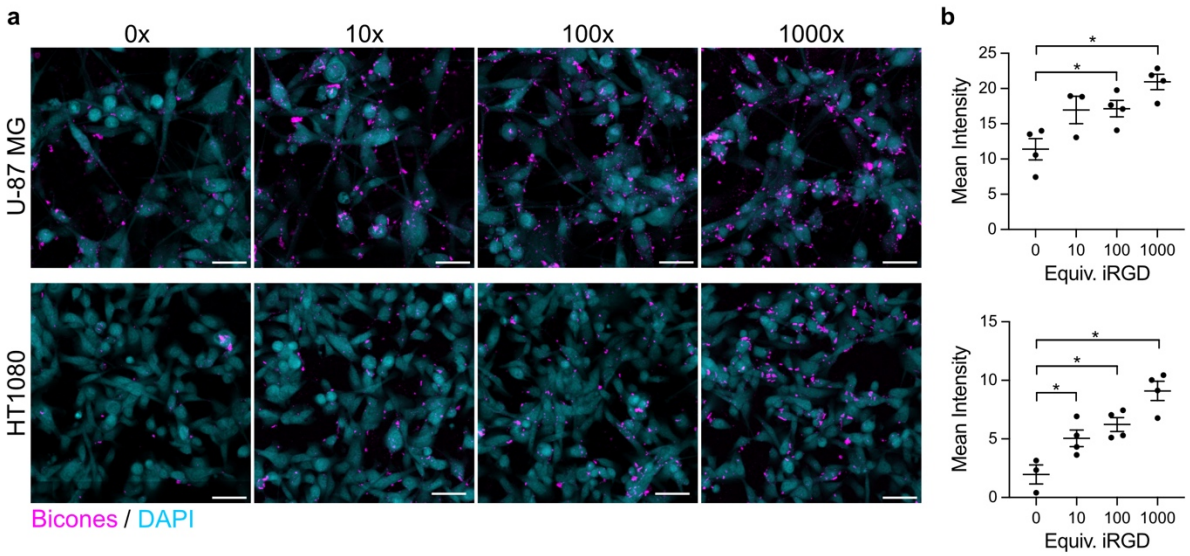

Figure S11. Targeting improves with iRGD loading. **a)** Representative confocal microscopy images of cells after incubation with bicones carrying the indicated maximum stoichiometry of iRGD peptides. Scale bars, 50 μm. **b)** Mean fluorescence intensity in the bicone channel of cell regions in images from panel A. U-87 MG (top) and HT-1080 (bottom) cells were defined by thresholding on autofluorescence in the DAPI channel. *N* = 4. Error bars, ± SEM. Welch's t-test, (*, $p < 0.05$).

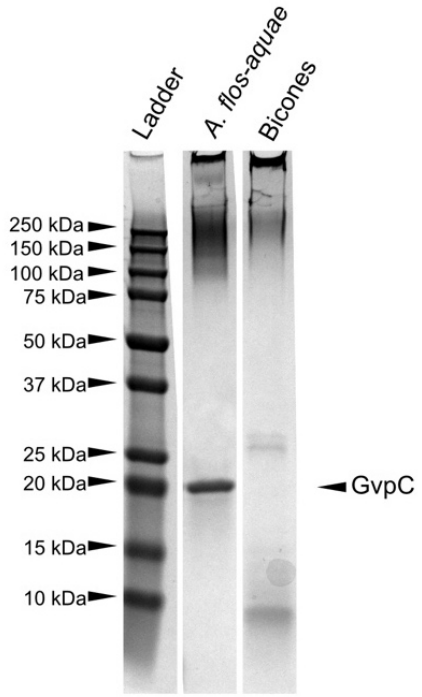

Figure S12. SDS-PAGE of bicones (200 µg mL^{-1}) and *Anabaena* GVs (OD 10). GvpC (indicated with an arrow) is not found on bicones.

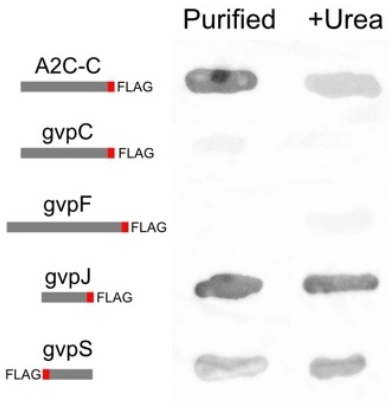

Figure S13. Anti-FLAG dot blot of purified bicones containing the indicated FLAG-fusion protein before and after treatment with 6 M urea to remove surface-bound proteins.

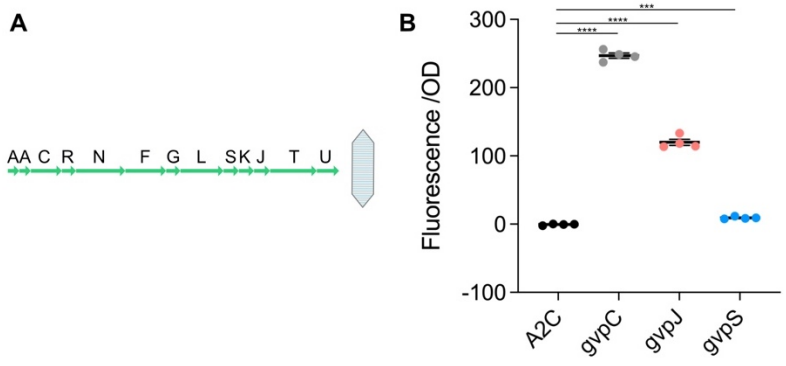

Figure S14. GvpJ and GvpS can also be used to genetically functionalize larger GVs. **a)** A2C gene cluster. The SpyTag peptide was appended to the end of gvpC, gvpJ, or gvpS. Purified particles were then reacted with SC-mNG. **b)** Fluorescence of purified samples after conjugation. *N* = 4. Error bars, ± SEM. Welch's t-test (***, p < 0.001; ****, p < 0.0001).

	Bicones	**Anabaena**
Length (nm)	72	519
Diameter (nm)	40	85
Total volume (aL)	0.03	2.784
Gas vol/total vol	0.764	0.903
Particles/mg protein	1.01e14	2.65e12 (~OD27 in 1 mL)
Acoustic Collapse Midpt (MPa)	~2.4	~0.9
Hydrostatic Collapse Midpt (MPa)	~1.2	~0.6

Table S1. Physical properties of bicones compared to *Anabaena* GVs.

		Forward	Reverse
gvpC	SpyTag	TAAGCCGACGAAGGGAGGATCTGGGATTTCTTTAATGGCAAAAATCC	tatgcgtctaccattacaatatgtgcCATGAAGTTCTCCAAAAAATAG
	FLAG	gataaaggggctctgggATTTCTTTAATGGCAAAAATCC	gtcatcatctttataatcCATGAAGTTCTCCAAAAAATAG
	deletion	GAGAACTTCTAAAGATCTAACTATTGGAGGCTACTAAAAATG	CAAAAAATAGTAAATTAGCGCTAGCAAG
gvpR	SpyTag		
	FLAG	gataaaggggctctgggGAAATTAAAAAAATTATGCAAGC	gtcatcatctttataatcCATTTTTAGTAGCCTCCAATAG
	deletion	GCGATAAGATGGCAGGAGCTTG	CTTTAGTAGCCTCCAATAGTTAGATCTTTATTAACC
gvpF	FLAG	gatgatgacaaaTAACGTGCTTCACAAATTAG	gtctttataatccccagagcccccTTTCTCTTCTACTTTTAGGC
	deletion	cgtgcttcacaaattagtaaccgc	GTTTTCAAGCTCCTGCCATCTTATC
gvpG	FLAG	aaagacgatgatgacaaaTAGATGGGAGAATTACTG	ataatccccagagcccccGGATTCCTCATTTCTTTTTTG
	deletion	GAGAAATAAATGGGAGAATTACTGTATTTATACGG	CTCTACTTTTAGGCGAATGTTCAC
gvpL	FLAG	gataaaggggctctgggGGAGAATTACTGTATTTATACG	gtcatcatctttataatcCATCTAGGATTCCTCATTTC
	deletion	CGTGAGGAATTAACATTATGTCTCTTAAAC	CTAGGATTCCTCATTTCTTTTTTGTGTTAGCTCTTC
gvpS	SpyTag	TAAGCCGACGAAGGGAGGATCTGGGTCTCTTAAACAATCCATGG	tatgcgtctaccattacaatatgtgcCATAATGTTAATTCCTCACTTTAC
	FLAG	gataaaggggctctgggTCTCTTAAACAATCCATGG	gtcatcatctttataatcCATAATGTTAATTCCTCACTTTAC
	deletion	gatgcaaccggtcagc	gtgttaattcctcactttacgc
gvpK	FLAG	GATGATGACGATAAATAAGCGGTCAGTAGGAGGAAC	CTTGTAATCCCCAGAGCCCCCAAGCAGGCTGCCTAGCGG
	deletion	cggtcagtaggaggaacag	gtcaggatccaagtggattcg
gvpJ	SpyTag	GTAGACGCATATAAGCCGACGAAGTAAAAACTGTACGCTACTTAAAAAA	CATTACAATATGTGCCCCAGATCCTCCACGTTTCGTTTCTATTTT
	FLAG	aaagacgatgatgacaaaTAAAAACTGTACGCTACTTAAAAAATG	ataatccccagagcccccACGTTTCGTTTCTATTTTTTC
	deletion	gaactgtacgctacttaaaaaatg	cctgttcctcctactgac
gvpT	FLAG	gataaaggggctctgggGCAACTGAAACAAAATTAGATAAC	gtcatcatctttataatcCATTGTAAATCCCTCCATTTTTTAAG
	deletion	gacgtaaaggaggaaagaaag	ggtaaatccctccatttttttaagtag
gvpU	FLAG	gataaaggggctctgggAGTACAGGCCCTTCTTTTTC	gtcatcatctttataatcCATGTCTTTCTTTCCTCCTTTAC
	deletion	GTCTTTCTTTCCTCCTTTACGTC	CAAACGGCGGGGGTGATTGC

Table S2. Primers used for appending SpyTag and FLAG tags, or for gene deletion.

References

1. Bourdeau, R. W. *et al.* Acoustic reporter genes for noninvasive imaging of microorganisms in mammalian hosts. *Nature* **553**, 86–90 (2018).
2. Lakshmanan, A. *et al.* Preparation of biogenic gas vesicle nanostructures for use as contrast agents for ultrasound and MRI. *Nat. Protoc.* **12**, 2050–2080 (2017).
3. Farhadi, A. *et al.* Recombinantly expressed gas vesicles as nanoscale contrast agents for ultrasound and hyperpolarized MRI. *AIChE J.* **64**, 2927–2933 (2018).